Energy Conversion and Management 86 (2014) 1118–1127

Contents lists available at ScienceDirect

Energy Conversion and Management

journal homepage: www.elsevier.com/locate/enconman

Integrated scheduling of renewable generation and demand response programs in a microgrid

Mohammadreza Mazidi [a], Alireza Zakariazadeh [a], Shahram Jadid [a], Pierluigi Siano [b,*]

[a] Electrical Engineering Department, Iran University of Science and Technology (IUST), Tehran, Iran
[b] Department of Industrial Engineering, University of Salerno, Fisciano, Italy

ARTICLE INFO

Article history:
Received 12 March 2014
Accepted 24 June 2014

Keywords:
Microgrid
Demand response
Stochastic optimization
Renewable generation
Reserve

ABSTRACT

Wind and solar energy introduced significant operational challenges in a Microgrid (MG), especially when renewable generations vary from forecasts. In this paper, forecast errors of wind speed and solar irradiance are modeled by related probability distribution functions and then, by using the Latin hypercube sampling (LHS), the plausible scenarios of renewable generation for day-head energy and reserve scheduling are generated. A two-stage stochastic objective function aiming at minimizing the expected operational cost is implemented. In the proposed method, the reserve requirement for compensating renewable forecast errors is provided by both responsive loads and distributed generation units. All types of customers such as residential, commercial and industrial ones can participate in demand response programs which are considered in either energy or reserve scheduling. In order to validate the proposed methodology, the proposed approach is finally applied to a typical MG and simulation results are carried out.

1. Introduction

Increasing penetration of renewable energy generation in electric grid implies that system operators will need to manage the variable and uncertain nature of renewable resources like wind and solar in order to continuously maintain the electricity generation and consumption balance [1,2]. This requires operational changes and procurement of greater quantities of various ancillary services. Traditionally, many of these power system services have been provided exclusively by generators. However, over the past decade, alternative resources like demand response have become increasingly capable of providing a greater number and quantity of such electric grid services [3,4].

Microgrid (MG), as a small part of a power system, is a low voltage distribution network, comprising various Distributed Generators (DG), storage devices, and controllable loads, that faces with intermittent renewable power generation management [5]. Regarding the credibility of MGs, in recent years, there have been several research projects on the design, control, and operation of MGs throughout the world, such as the CERTS microgrid in USA [6,7], the smart poly-generation microgrid pilot project of the University of Genoa in Italy [8], and the energy integration test project carried out by NEDO in Japan [9]. As with all new technologies, the initial price of MGs is going to be expensive, but when they will built in scale and the cost of solar, wind, and other renewables will continue to fall, MGs will become increasingly cost-effective as well as efficient. Financial benefits of MGs may be observed as direct economic benefits, impacting both the capital and operating costs of the power system, or less directly, as service and environmental benefits [10,11].

However, the optimization of a MG has important differences from the case of a large power system and its conventional energy and reserve scheduling problem [12]. The control and scheduling of Distributed Energy Resources (DERs), including renewable generation in a MG, have been studied in many works [13–15]. A dynamic modeling and control strategy for a sustainable MG primarily supplied by wind and solar energy has been presented in [16]. The study considered both wind energy and solar irradiance changes in combination with load power variations.

Focusing on uncertainty of renewable sources, the wind speed and solar irradiance forecasting problem in a MG has been investigated in [17,18]. In [17], an artificial neural network has been used to forecast wind speed and optimal set points of DERs and storage devices have been determined based on the forecasted data in such a way that the total operation cost and the net emissions are simultaneously minimized. In [18], a day-ahead power forecasting module has been presented in order to provide the Photovoltaic

* Corresponding author. Tel./fax: +39 089964294.
E-mail addresses: mr.mazidi@ee.iust.ac.ir (M. Mazidi), zakaria@iust.ac.ir (A. Zakariazadeh), jadid@iust.ac.ir (S. Jadid), psiano@unisa.it (P. Siano).

http://dx.doi.org/10.1016/j.enconman.2014.06.078
0196-8904/

(PV) output data for DER scheduling in a MG. However, providing reserve for compensating wind and PV power fluctuations has not been taken into account within the day-ahead DER scheduling. A stochastic programming approach for reactive power scheduling of a MG, considering the uncertainty of wind power has been presented in [19]. Monte Carlo simulation enhanced by scenario reduction technique has been used to simulate plausible states of wind power and find an optimal operating strategy of DGs. In [20], MG intelligent energy management under cost and emission minimization has been investigated. Moreover, a fuzzy logic expert system has been implemented for battery scheduling. The proposed approach can handle uncertainties regarding the fuzzy environment of the overall MG operation and the uncertainty related to the forecasted parameters. The estimation model of spinning reserve requirement in a MG was proposed in [21]. In the proposed method, the uncertainty of wind and solar generation, as well as the unreliability of units and uncertainties caused by load demand, are considered. The approach aggregated various uncertainties in order to reduce the computational burden. The demand side reserve and load participation in energy markets was not considered in the model. In [22], a method for modeling the output powers of renewable DGs by using historical data has been presented. The method provides hourly generation and load profile considering the intermittent nature of renewable generation. The power dispatch problem of DGs for optimal operation of a MG has been proposed in [23]. The reserve has been scheduled for variations in load demand and the power outputs of non-dispatchable DGs while the objective function aims at minimizing the fuel cost during the grid-connected and islanded modes. In [24,25], wind speed, solar irradiance and load demand in each hour have been modeled by probability distribution functions (PDFs). Then, PDFs are truncated into a limited number of states; every scenario in each day-ahead period consists of a state derived from wind speed, solar irradiance and load demand discrete PDFs.

The concept and role of Demand Response (DR) in providing reserve in a MG is very important, especially in presence of renewable sources. DR programs are used by electric utilities to manage customer electricity consumption in response to supply conditions. A number of methods such as demand management in building [26,27], heat pumps and battery storage system management [28] have been used to address DR programs in MGs. A real-time pricing scheme for residential load management was proposed in [29,30]. These papers presented an automatic and optimal scheme for the operation of each appliance in households in presence of a real-time pricing tariff.

In addition to participate in energy scheduling, DR programs are being investigated for providing ancillary services such as primary frequency regulation [31,32], spinning reserve [33–35], real time voltage control [36] and system security improvements [37]. Basically, there are two typical approaches: indirect load control [38] and direct load control [39]. The potential of DR in balancing supply and demand on an hourly basis has been investigated in [40]. Results indicated that DR has the potential to improve overall power system operation, with production cost savings arising from both improved thermal power plant operation and increased wind production. Moreover, DR resources present a potentially important source of grid flexibility and can support intermittent renewable generation integration. The operation of an electrical demand side management system in a real solar house has been presented in [41]. Experimental results showed that a combination of DR and PV generation allows the use of local control techniques and achieves energy efficient levels.

However, analyses on renewable sources integration have not been explicitly incorporated as reserve capacity in the MG model.

In this paper, Latin hypercube sampling (LHS) is used in order to model plausible wind and PV generation scenarios. Using a stochastic method, energy and reserve scheduling is carried out by considering the generated scenarios. Moreover, the proposed method enables all type of residential, commercial and industrial loads to provide reserve capacity as well as load demand reduction in presence of a DR program.

The rest of this paper is organized as follows. In Section 2 and 3 DR programs and renewable generations' uncertainty are modeled, respectively. The method formulation is detailed in Section 4. Simulation results are presented in Section 5 while the paper is concluded in Section 6.

2. Demand response participants

Different types of electricity customers with different electricity consumption behavior and pattern are considered in the proposed method. The types of customers and their involvement in DR programs are described in this section:

2.1. Industrial customer

Industrial customers are usually characterized by heavy loads and have the largest load demand among residential and commercial customers. As every factory comprises more than one production line, the energy curtailment in each production line has a distinct price offer pertaining to its production. So, industrial customers offer their load curtailment as a multi steps package. The equations used for modeling the behavior of the ith industrial customer are the following ones from (1-4).

$$L^i_{Min} \leqslant l^i_1 \leqslant L^i_1 \tag{1}$$

$$0 \leqslant l^i_k \leqslant \left(L^i_{k+1} - L^i_k\right) \quad \forall\ k = 2,3,\ldots,K \tag{2}$$

$$IC^E(i,t) = \sum_k l^i_k \tag{3}$$

$$IP^E(i,t) = \sum_k o^i_k \cdot l^i_k \tag{4}$$

where $i = 1, 2, \ldots, I$ represents an index used to identify industrial customers; index $k = 1, 2, \ldots, K$ represents the step of price-quantity offer package; l^i_k and o^i_k are the accepted load reduction and the offer price of industrial customer i in step k of price-quantity offer package; L^i_k is the maximum load reduction of industrial customer i in step k; L^i_{Min} is the minimum load reduction that an industrial customer can carry out; $IC^E(i,t)$ and $IP^E(i,t)$ are the total scheduled load reduction quantity and related cost prepared by the industrial customer i in period t.

At each hour, the sum of the scheduled energy reduction and reserve provided by each industrial load should not be greater than its maximum load reduction offer (L^i_{Max}). This means that the uncommitted load reduction capacity of each industrial customer's offer package in the energy scheduling can be scheduled for the reserve requirement. The reserve provided by each industrial customer is calculated as follows:

$$IC^E(i,t) + IC^R(i,t) \leqslant L^i_{Max} \tag{5}$$

$$IP^R(i,t) = IC^R(i,t) \times q^R_{i,t} \tag{6}$$

where t represents index of optimization period; $IC^R(i,t)$, $IP^R(i,t)$ represent the scheduled reserve and its cost provided by industrial customer i in period t, respectively; $q^R_{i,t}$ is price offer for providing reserve.

2.2. Commercial customer

Commercial consumers always offer the maximum amount of possible load reduction at the desired price for curtailment. The equations used for modeling the behavior of the commercial customer b, participating in both energy reduction and reserve commitment are given as follows:

$$CC^E(b,t) + CC^R(b,t) \leqslant CC^{max}_{b,t} \tag{7}$$

$$CP^E(b,t) = CC^E(b,t) \times q^E_{b,t} \tag{8}$$

$$CP^R(b,t) = CC^R(b,t) \times q^R_{b,t} \tag{9}$$

where $b = 1, 2, \ldots, B$ represents index of commercial customers, $CC^E(b,t)$ and $CC^R(b,t)$ are the scheduled load reduction and reserve provided by commercial customer b in period t; $CC^{max}_{b,t}$ represents the maximum quantity of load reduction offered by commercial consumer b in period t. $q^E_{b,t}$ and $q^R_{b,t}$ are the price offer of commercial customer b for energy reduction and the committing reserve in period t, respectively; $CP^E(b,t)$ and $CP^R(b,t)$ are the cost due to load reduction and committing reserve provided by commercial customer b in period t.

2.3. Residential customer

Due to the highest energy demand in the industrial and commercial sector, most of researches have been focused on energy management in this area. However, the residential sector should be also considered, as this sector is the one that experiences the strongest increase of load demand. Moreover, because of the number of users in the residential sector, its consumption is increasing in recent years, reaching the 28.8% of the total electricity consumption in the EU [42]. Therefore, the energy management in the residential sector is an important task for the power system operators, as already shown in [43].

In this paper, the residential customer is allowed providing load curtailing or shifting if involved in DR programs. Constraints (10) show that sum of energy reduction and reserve commitment of each residential customer at every hour should be lower or equal to the maximum amount of its offers. The equations used for modeling the behavior of the hth residential customer are the following ones.

$$RC^E(h,t) + RC^R(h,t) \leqslant RC^{max}_t \tag{10}$$

$$RP^E(h,t) = RC^E(h,t) \times q^E_{h,t} \tag{11}$$

$$RP^R(h,t) = RC^R(h,t) \times q^R_{h,t} \tag{12}$$

where $h = 1, 2, \ldots, H$ represents index of residential customers (home); $RC^E(h,t)$ and $RC^R(h,t)$ are the scheduled load reduction and the reserve provided by residential customer h in period t. RC^{max}_t represents the maximum quantity of load reduction offered by residential customer h in period t; $q^E_{h,t}$ and $q^E_{h,t}$ the price offer of residential customer h for energy and committing reserve in period t, respectively; $RP^E(h,t)$ and $RP^R(h,t)$ represent the cost due to load reduction and committing reserve provided by residential customer h in period t.

The shiftable appliances constraint which shows the time limitation of their performance is given as follows:

$$\sum_{t=\tau s}^{\tau e} d(t,h,ty) = \tau w \tag{13}$$

$$HDA(t,h,ty) = \sum_{\tau w} d(t,h,ty) \times P^{Nom}_{h,ty} \tag{14}$$

where indices h and ty represent the hth residential customer and the tyth shiftable appliance, respectively; $P^{Nom}_{h,ty}$ is the nominal power consumption of shiftable appliances ty at home h that turn on in period t ($\tau s \leqslant t \leqslant \tau e$); $d(t,h,ty)$ is on/off status (1/0) of home appliances ty at home h and in period t. For shiftable load scheduling, τs and τe represent the desired start and end time of the shiftable appliances working period, respectively, and τw is the working period. Also, it is assumed that the working period of the shiftable appliances cannot be interrupted.

3. Uncertainty modeling of renewable generation

It is assumed that wind turbines and PV units are installed in the MG. As the wind and solar have a probabilistic nature, the output power of these units is intermittent. To model the uncertainties related to wind and PV generation, two probability density functions are implemented.

3.1. Wind generation modeling

The Rayleigh probability density function (PDF) is regularly used as a proper expression model of wind speed behavior in each forecasted period [44]. Rayleigh PDF is a special case of Weibull PDF in which the shape index is equal to 2.

$$f_w(v) = \left(\frac{2v}{c^2}\right) \exp\left[-\left(\frac{v}{c}\right)^2\right] \tag{15}$$

where $f_w(v)$, c and v are Rayleigh PDF, scale index and wind speed, respectively. If the mean value of the wind speeds (v_m) for a site is known, then the scaling index c can be calculated as shown in (16) and (17):

$$v_m = \int_0^\infty v f_w(v) dv = \int_0^\infty \left(\frac{2v^2}{c^2}\right) \exp\left[-\left(\frac{v}{c}\right)^2\right] dv = \frac{\sqrt{\pi}}{2} c \tag{16}$$

$$c \simeq 1.128 v_m \tag{17}$$

The output power of the wind turbine is calculated using the wind turbine power curve parameters as described by Eq. (18).

$$P_w(v) = \begin{cases} 0, & 0 \leqslant v_{aw} \leqslant v_{ci} \\ P_{rated} \times \frac{(v_{aw} - v_{ci})}{(v_r - v_{ci})}, P_{rated} & v_{ci} \leqslant v_{aw} \leqslant v_r \\ 0, & v_{co} \leqslant v_{aw} \end{cases} \tag{18}$$

where v_{ci}, v_r and v_{co} are the cut-in speed, rated speed and cut-off speed of the wind turbine, respectively.

3.2. Solar generation modeling

The output of PV mainly depends on irradiance. The distribution of hourly irradiance at a particular location usually follows a bimodal distribution [45,46], which can be seen as a linear combination of two unimodal distribution functions [47]. A Beta PDF is utilized for each unimodal [13,15], as set out in the following:

$$f_b(si) = \begin{cases} \frac{\Gamma(\alpha+\beta)}{\Gamma(\alpha)\Gamma(\beta)} \times si^{(\alpha-1)} \times (1-si)^{(\beta-1)} & \text{for } 0 \leqslant si \leqslant 1, \alpha \geqslant 0, \beta \geqslant 0 \\ 0 & \text{otherwise} \end{cases} \tag{19}$$

where si represents the solar irradiance (kW/m^2). To calculate the parameters of the Beta distribution function (α, β), the mean (μ) and standard deviation (σ) of the random variable are utilized as follows:

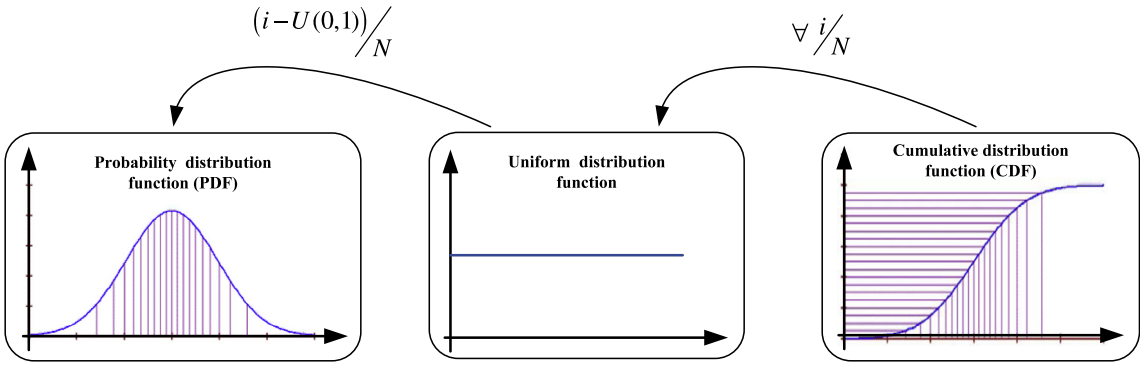

Fig. 1. The procedure in Latin hypercube sampling method.

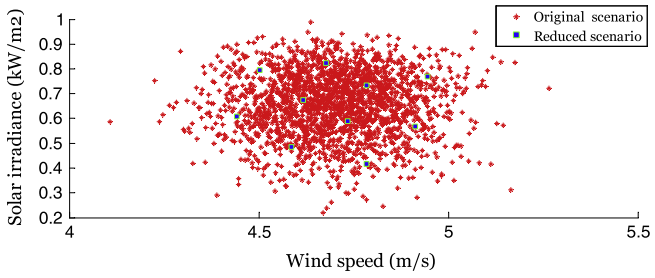

Fig. 2. The original and reduced scenario by *K*-means clustering algorithm.

$$\beta = (1-\mu)\times\left(\frac{\mu\times(1+\mu)}{\sigma^2}-1\right) \tag{20}$$

$$\alpha = \frac{\mu\times\beta}{1-\mu} \tag{21}$$

Given the irradiance distribution and irradiance-to-power conversion function, the PV power distribution can be obtained. The irradiance-to-power conversion function used in this paper is similar to that used in [48]:

$$P_{pv}(si) = \eta^{pv}\times S^{pv}\times si \tag{22}$$

where $P_{pv}(si)$ represents PV output power (kW) for irradiance si; η^{pv} and S^{pv} are the efficiency (%) and total area (m^2) of PV, respectively.

3.3. Scenario generation

In this paper, the Latin hypercube sampling (LHS) is implemented in order to combine and generate scenarios of wind and solar power generations. The LHS method offers great benefits in terms of increased sampling efficiency and faster run time compared to the traditional Monte Carlo sampling method [49]. As a result, LHS method is used to generate samples of wind speed and solar irradiation. The LHS method is divided into two steps including sampling and combination. In the sampling step, 4000 samples are generated to represent the stochastic nature of wind speed and solar irradiation. For this end, the cumulative distribution function of wind speed and solar irradiation are divided into 4000 intervals with equal probability of 1/4000. Then for each random variable, i.e., wind speed and solar irradiation, the following procedure, as shown in Fig. 1, is applied.

For i = 1 to 4000 **DO**

Step 1: A value is randomly selected from each interval. The sampled cumulative probability at interval ith is:

$$Prob_i = \left(\frac{1}{4000}\right)r_u + \frac{(i-1)}{4000} \tag{23}$$

where $r_u \in (0,1)$ is a uniformly distributed random number.

Step 2: The sampled value is transformed into the value x_i using the inverse of the distribution function F^{-1}:

$$x_i = F^{-1}(Prob_i) \tag{24}$$

END FOR

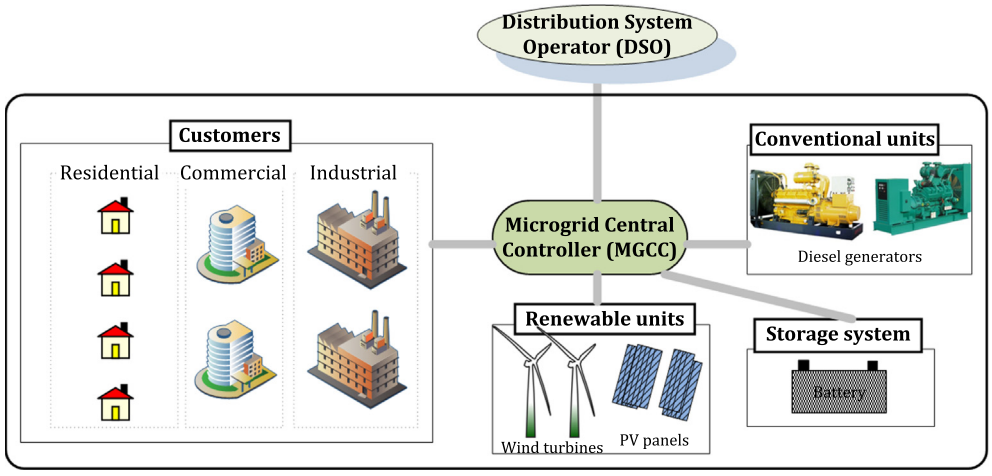

Fig. 3. Typical microgrid test system.

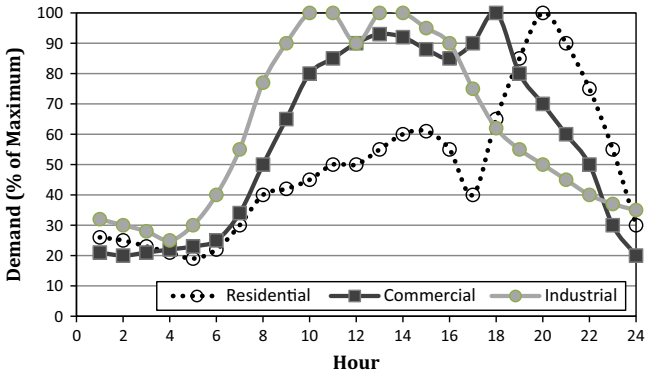

Fig. 4. Daily load curves for the three load types of The MG.

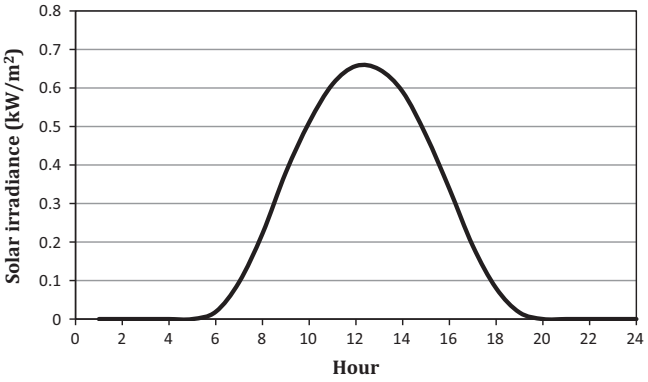

Fig. 6. Mean value of hourly solar irradiance.

Table 1
The technical and economical features of diesel generators.

Unit	Cost coefficient			Technical constraints		
	a_j ($)	b_j ($/kW h)	c_j ($/kW h^2)	Startup ($)	P_{min} (kW)	P_{max} (kW)
DG1	0.184	0.091	0.0061	0.15	30	300
DG2	0.221	0.142	0.0056	0.21	40	400

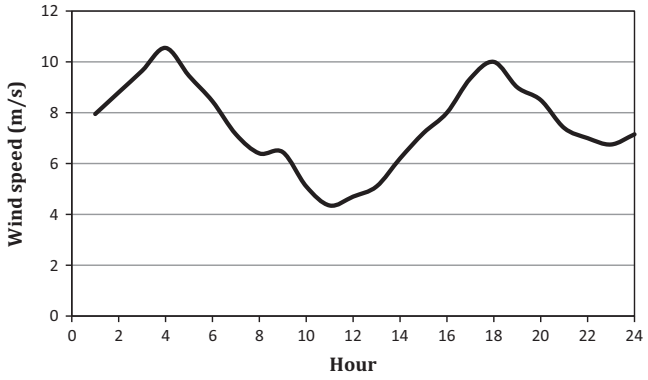

Fig. 5. Mean value of hourly wind speed.

Table 2
Standard deviations of solar irradiance and wind speed.

Hour	Solar σ	Wind σ	Hour	Solar σ	Wind σ
1	–	0.021	13	0.282	0.179
2	–	0.047	14	0.265	0.235
3	–	0.078	15	0.237	0.292
4	–	0.114	16	0.204	0.347
5	–	0.128	17	0.163	0.430
6	0.035	0.137	18	0.098	0.487
7	0.110	0.135	19	0.032	0.463
8	0.182	0.139	20	–	0.460
9	0.217	0.157	21	–	0.421
10	0.253	0.138	22	–	0.417
11	0.273	0.129	23	–	0.420
12	0.284	0.152	24	–	0.464

Table 3
Hourly price of open market.

t	1	2	3	4	5	6
$/MW h	47.47	31.64	31.65	32.60	40.78	38.64
t	7	8	9	10	11	12
$/MW h	158.95	384.14	67.27	52.29	44.59	108.49
t	13	14	15	16	17	18
$/MW h	60.64	40.88	28.50	38.75	35.55	112.42
t	19	20	21	22	23	24
$/MW h	575.58	87.72	35.06	47.18	61.27	33.90

Table 4
Price-quantity offer package for kW industrial customers (IC).

	Quantity (kW) Price (Cent/kWh)			
IC1	0–5 7	5–10 15	10–50 29	50–70 41
IC2	0–5 5	5–20 7.5	20–30 31	30–60 49

The Cholesky decomposition method is adopted to combine the sampled values of wind speed and solar irradiation because this method gives the smallest correlation coefficients between variables [50].

3.4. Scenario reduction technique

In stochastic programming, when the number of scenarios increases, the runtime will also raises. It is a problem for this approach, since for 24-h scheduling of energy and reserve, the operator has to decide as fast as possible. An efficient scenario reduction method is therefore required in order to decrease the computational time required for simulating a large number of scenarios [50]. In this paper, *K*-means clustering algorithm as clarified in [51] is selected to reduce the number of scenarios. The aim of this algorithm is to arrange original scenarios of wind speed and solar irradiation into clusters according to similarities. The centroid of each cluster is defined as the mean value of wind speed and solar irradiation allocated to each cluster. According to this definition, the *K*-means algorithm is based on the iterative procedure described below:

1: Select the number of required clusters based on the specific problem.
2: Assign the initial centroid of each cluster randomly.
3: **WHILE** change in the cluster compositions becomes small
4: Calculate the distances between each original scenario and each cluster centroid.
5: Assign each original scenario to the closest cluster based on distances calculation in 3.

Table 5
Commercial customers (CC) load reduction offer.

Hour	CC1		CC2	
	Maximum Reduction (kW)	Price (kW h)	Maximum Reduction (kW)	Price (kW h)
8	15	6	12	14
9	9	7	24	9
10	5	4	5	12
13	7	10	–	–
14	7	50	–	–
15	21	60	16	12
16	7	8.5	19	8
17	10	6	25	60
18	4	10	18	60
19	15	20	10	30
20	28	30	18	10
21	10	30	21	6
22	3	30	8	20
23	6	30	–	–

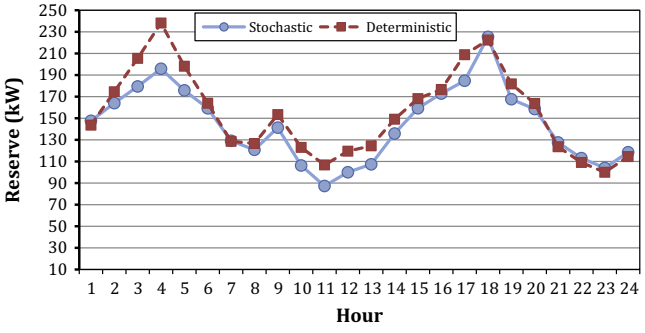

Fig. 7. Reserve requirements in the stochastic and deterministic methods.

6: Calculate new cluster centroids using the original scenarios assigned to each cluster.
7: **END WHILE**

Each cluster represents a scenario which consists of two different values, i.e. mean value of wind speed and solar irradiation. The number of each cluster scenarios divided by the total number of original scenarios provides the probability of each scenario, π_s, that reflects its possibility of occurrence in the future. An example of scenario reduction is shown in Fig. 2.

4. Stochastic scheduling formulation

In order to perform day-ahead energy and reserve scheduling, the Microgrid Central controller (MGCC) receives and stores information from responsive loads and DGs (renewable and conventional units) and the electricity market.

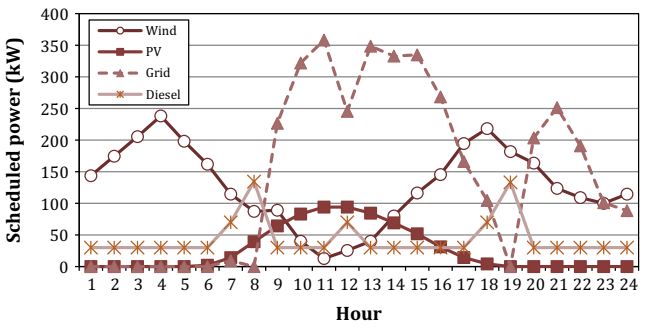

Fig. 8. Scheduled energy without DR.

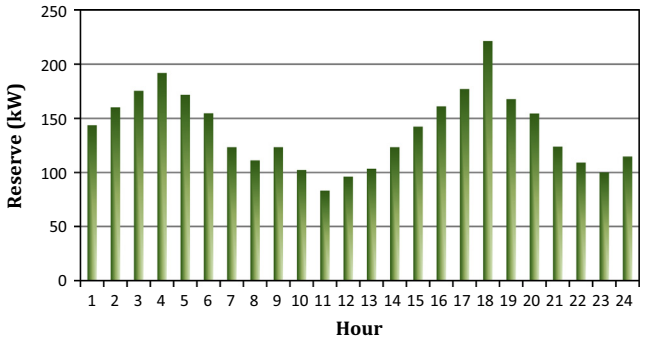

Fig. 9. Scheduled reserve provided by diesel generators without DR.

4.1. Objective function

To model the wind and PV power generations' uncertainties within the MG energy and reserve scheduling, a two-stage stochastic programming framework is developed. A two-stage stochastic microgrid energy scheduling model allows making an optimal decision on the day-ahead energy and reserve transactions in the first stage while considering the real-time operations with the wind/solar power variability in the second stage. By using the proposed two-stage stochastic framework, the day-ahead energy and reserve scheduling are determined in the first stage with the objective to identify the optimal amount of electricity to be purchased from the main grid and the commitment of DG units over the next 24 h. These first-stage decision variables do not belong to a specific scenario. On the other hand, the variables in the second stage are related to scenarios and vary with scenarios.

As the power output of wind and solar generating units in one scenario is different from another, the purchased power from the main grid and non-renewable DG units, as well as load curtailments, change in each scenario in order to keep the balance between generation and consumptions. Therefore, based on each scenario, the new set points for each energy sources are determined. The objective function *EC*, that should be minimized, represents the expected operational cost in the MG mode over the next 24 h [52,53].

As shown in the objective function, the second-stage variables are distinguished by index *s* that shows the corresponding scenario. Also, the second-stage terms are multiplied by the probability of scenarios π_s in order to reflect the likelihood of each scenario in scheduling results.

$$EC=\sum_{t=1}^{T}\Bigg[P_g(t)\times\rho_E^t+\sum_{j=1}^{J}\Big\{C_{DG}(j,t)+R_{DG}(j,t)\times q_j^R+SU(j,t)\Big\}+\sum_i IP^E(i,t)+IP^R(i,t)+\sum_b CP^E(b,t)+CP^R(b,t)+\sum_h RP^E(h,t)+RP^R(h,t)\Big]+\sum_{s=1}^{S}\pi_s\Bigg\{\sum_{t=1}^{T}\Bigg[P_g^s(t,s)\times\rho_E^t+\sum_{j=1}^{J}C_{DG}^s(j,t,s)+\sum_{b=1}^{B}CP^s(b,t,s)+\sum_{i=1}^{I}IP^s(i,t,s)+\sum_{h=1}^{H}RP^s(h,t,s)+E(s,t)\times V_t\Bigg]\Bigg\}\tag{25}$$

In the first-stage part of the objective function, $P_g(t)$ and ρ_E^t respectively represent, the scheduled purchased energy from the main grid and hourly electricity price of the market in period t; $j = 1, 2, \ldots, J$ is the index of non-renewable DGs; $C_{DG}(j,t)$, $R_{DG}(j,t)$, q_j^R and $SU(j,t)$ are the hourly fuel cost, committed reserve, reserve price and start-up cost of non-renewable DG j in period t, respectively; $IP^E(i,t)$, $CP^E(b,t)$ and $RP^E(h,t)$ represent the costs due to load reduction provided by industrial, commercial and residential customers in period t, respectively; $IP^R(i,t)$, $CP^R(b,t)$ and $RP^R(h,t)$ represent the cost due to committing reserve provided by industrial, commercial and residential customers in period t, respectively.

In the second-stage part of the objective function, π_s is the probability of scenario s. $C_{DG}^s(j,t,s)$ represents the hourly fuel cost of non-renewable DG j in period t and scenario s; $IP^s(i,t,s)$, $CP^s(b,t,s)$, and $RP^s(h,t,s)$ represent the cost due to required load reduction provided by industrial, commercial and residential customers in period t and scenario s, respectively; $E(s,t)$ represents the amount of involuntarily load shedding in period t and scenario s; V_t represents the value of lost load in period t. The involuntarily load shedding is used in this model to prevent committing more reserve in some scenarios with low probability [54].

The fuel cost of a generator can be generally expressed as a function of its real power output and can be modeled by a quadratic polynomial [55]. The operational cost of a distributed generation unit (like a diesel generator) with a quadratic cost function $C_{DG}(j,t)$ is given by [56]:

$$C_{DG}(j,t)=a_j\times u(j,t)+b_j\times P_{DG}(j,t)+c_j\times P_{DG}^2(j,t)\tag{26}$$

where $P_{DG}(j,t)$ represents the scheduled active output power of non-renewable DG j in period t; a_j, b_j and c_j represent the cost coefficient of DG j.

To implement a linear programming approach, the non-linear cost function of DG is approximated by a linear function that for practical purpose is indistinguishable from the nonlinear model [57]. This method is detailed in [34].

4.2. Constraints

The constraints of the stochastic optimization method are described below:

4.2.1. Load balance

$$P_g(t)+\sum_{j=1}^{J}P_{DG}(j,t)+\sum_{w=1}^{W}P_w^t+\sum_{pv=1}^{PV}P_{pv}^t+\eta^+\times P_B^+(t)-P_B^-(t)=P_L(t)-\sum_i IC^E(i,t)-\sum_h RC^E(h,t)-\sum_b CC^E(b,t)\quad\forall\ t\tag{27}$$

where P_w^t and P_{pv}^t represent the mean values of wind power of wind turbine w and the solar power of PV unit pv in period t, respectively; $P_B^+(t)$ and $P_B^-(t)$ represent the scheduled battery discharge and charge power in period t, respectively; η^+ represents the battery charge efficiency coefficients; $P_L(t)$ and $Loss(t)$ represent the total hourly demand and total network losses in period t, respectively; $IC^E(i,t)$, $CC^E(b,t)$ and $RC^E(h,t)$ represent the scheduled load reductions quantity prepared by the industrial, commercial and residential customers in period t, respectively.

The energy balance at each scenario should also be satisfied.

$$P_g(t)+\sum_{j=1}^{J}P_{DG}^s(j,t,s)+\sum_{w=1}^{W}P_w^s(s,t)+\sum_{pv=1}^{PV}P_{pv}^s(s,t)+\eta^+\times P_B^+(t)-P_B^-(t)=P_L(t)-\sum_i IC^s(b,t,s)-\sum_b CC^s(i,t,s)-\sum_s RC^s(h,t,s)-E(s,t)\quad\forall\ t,s\tag{28}$$

where $P_{DG}^s(j,t,s)$ represents the active output power of non-renewable DG j in period t and scenario s; $P_w^s(s,t)$ and $P_{pv}^s(s,t)$ represent, respectively, the output power of wind turbine w and of PV system pv in period t and scenario s; $IC^s(i,t,s)$, $CC^s(b,t,s)$ and $RC^s(h,t,s)$ represent the required load reduction quantity prepared by the industrial, commercial and residential customers in period t and scenario s, respectively.

4.2.2. Demand response participants' constraints

The scheduled reserves offered by Industrial ($IC^R(t)$), commercial ($CC^R(t)$) and residential ($RC^R(t)$) customers at each hour are defined as the additional load demand reduction of each customer in each scenario if compared to its scheduled load demand reduction. The selection of the maximum value guarantees that the scheduled load reserve can cover load reduction's requirement in all scenarios. In other words, the reserve provided by a customer is the largest amount of load reduction deviation in all possible scenarios away from the scheduled ones.

$$IC^R(i,t)\geqslant IC^s(i,t,s)-IC^E(i,t)\quad\forall\ s,i,t\tag{29}$$

$$CC^R(b,t)\geqslant CC^s(b,t,s)-CC^E(b,t)\quad\forall\ s,b,t\tag{30}$$

$$RC^R(h,t)\geqslant RC^s(h,t,s)-RC^E(h,t)\quad\forall\ s,h,t\tag{31}$$

Regarding Eqs. (29)–(31), the differences between load reductions in each scenario from their scheduled values represent the corrective actions required for each scenario. These corrective actions are carried out by using the scheduled reserve capacity. So, the additional load reduction in each scenario determines the required reserve.

The reactive power reduction of each load in the DR program is considered to be proportional to the active power reduction according to the power factor of the considered load.

4.2.3. Non-renewable DG power and reserve constraints

The non-renewable distributed generation units have a maximum and minimum generating capacity beyond which it is not feasible to generate due to technical reasons. Generating limits are specified as upper and lower limits for the real and reactive power outputs.

$$P_{DG}(j,t)+R_{DG}(j,t)\leqslant P_{DG,j}^{max}.u(j,t)\quad\forall\ j,t\tag{32}$$

$$P_{DG}(j,t)\geqslant P_{DG,j}^{min}.u(j,t)\quad\forall\ j,t\tag{33}$$

where $u(j,t)$ represents the on/off status (1/0) of the non-renewable DG j in period t; $P_{DG,j}^{max}$ and $P_{DG,j}^{min}$ are, respectively, the maximum and minimum output power limits of non-renewable DG j.

The start up cost ($SU(j,t)$) of DG units is calculated as follows:

$$SU(j,t)\geqslant Sc_j\times(u(j,t)-u(j,t-1))\tag{34}$$

$$SU(j,t)\geqslant 0\tag{35}$$

where Sc_j represents the start-up cost of non-renewable DG j.

The spinning reserves ($R_{DG}(j,t)$) provided by DG units are calculated as follows:

$$R_{DG}(j,t) \geqslant P^{s}_{DG}(t,s) - P_{DG}(j,t) \quad \forall\, j,t,s \tag{36}$$

Regarding the Eq. (36), the DG power output deviation in each scenario (P^{s}_{DG}) is compared to the scheduled one (P_{DG}) and the DG reserve (R_{DG}) is computed.

4.2.4. Battery charge and discharge constraints

The battery used in the MG cannot charge and discharge arbitrary. The following constraint should be considered for the scheduling program of the battery:

$$SOC(t) = SOC(t-1) + \eta^{-} \times P^{-}_{B}(t) - P^{+}_{B}(t) \tag{37}$$

$$SOC_{Min} \leqslant SOC(t) \leqslant SOC_{Max} \tag{38}$$

where $SOC(t)$ is the battery state of charge that defines how much energy is stored in it; η^{-} represents the battery charge efficiency coefficients; SOC_{Min} and SOC_{Max} represent, respectively, the minimum and maximum capacity of battery. Also the charge and discharge limit should be considered as follows:

$$P^{-}_{B}(t) \leqslant P^{-}_{B\_Max} \tag{39}$$

$$P^{+}_{B}(t) \leqslant P^{+}_{B\_Max} \tag{40}$$

$$X(t) + Y(t) \leqslant 1; X, Y \in \{0,1\} \tag{41}$$

where $P^{-}_{B\_Max}$ and $P^{+}_{B\_Max}$ represent the battery charge and discharge ramp rate limits, respectively; $X(t)$ and $Y(t)$ are the binary variables that model the battery charge and discharge state in each period.

5. Case study

The proposed model was tested on a typical MG depicted in Fig 3. Three types of customers are considered in the MG: one hundred of residential customers, two commercial and two medium industrial customers. The maximum electricity demand of the aggregated residential, commercial and industrial customers are 200 kW, 100 kW and 300 kW, respectively. Aggregated daily load curves for the three load types are shown in Fig. 4. The technical aspects of two diesel generators installed in the MG are obtained from [58,59] and shown in Table 1 while their cost function calculation is described in [60].The spinning reserve of DGs are priced at a rate equal to 20% of their highest marginal cost of the energy production [61].

The energy storage system consists of a battery with a capacity of 30 kW which charging and discharging ramp rate limits for each hour equal to 10 kW and 20 kW, respectively. Four wind turbines are installed in the test system, they are of the same type: 100 kW power rated with cut-in speed of 3 m/s, nominal speed of 12 m/s, and cut-out speed of 25 m/s [62]. Other specifications of the wind turbines are given in [62]. Ten 10 kW PV systems are considered in the MG: each of them is composed of 40 × 250 W solar panels with η = 18.6% and S^{PV} = 40 m^2 [63]. The mean values of hourly wind speed and solar irradiance are shown in Figs. 5 and 6 [64,65]. The variance of wind speed and solar irradiance is also given in Table 2 [65]. The VOLL that is needed to estimate the social cost caused by interruptions is taken as 1.5 $/kW h. The hourly energy price of Ontario electricity market on Wednesday 23 January 2013 [66] has been assumed as shown in Table 3. The industrial and commercial customers' price and amount of offers for load reduction is presented in Tables 4 and 5, respectively. It is assumed that forty percent of residential customers are willing to participate in DR programs during the scheduling horizon. In this case study, it has been assumed that each house has a demand curtailment capability of 500 W. Also, the residential customers participating in a DR program have a dishwasher and a washer dryer as shiftable appliances. The power consumption of the dishwasher and the washer/dryer are assumed to be 700 and 1200 W, respectively [67].

In order to show the advantage of stochastic optimization in allocating reserve for each period, the amount of scheduled reserve using the proposed stochastic method and conventional deterministic one has been compared in Fig. 7. In the deterministic approach, the amount of reserve requirement is assumed as 30% of the forecasted renewable power generation in each period [68,69].

As shown in Fig. 7, the scheduled reserve in the proposed stochastic method is lower than the one in the deterministic method. In the stochastic method, the amount of reserve is determined based on the probability of scenarios and the price of reserve. So, it is not preferred to allocate much reserve for a scenario with very low probability.

In order to analyze the effect of DR programs, the stochastic energy and reserve scheduling is carried out in two cases: with and without considering DR programs.

Figs. 8 and 9 show, respectively, the scheduled energy and reserve in the case without considering DR programs. As shown in Fig. 9, the diesel generator units provided all the reserve in each period. So, as illustrated in Fig. 8, one of the diesel generators must at least be turn on during all the scheduling period in order to provide the required spinning reserve. So, during the periods with high electricity prices, the diesel generators loose the chance to sell energy due to the necessity of providing spinning reserve and operator is forced to buy the energy form the main grid with a higher price. On the other hand, during the hours when the electricity prices are low, the diesel generator has been forced to turn on with a higher price due to the need of providing spinning

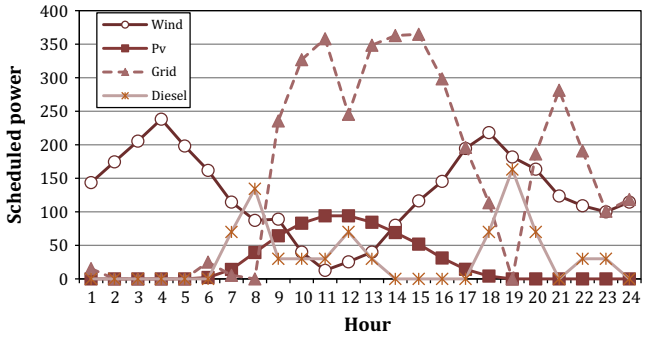

Fig. 10. Scheduled energy in the case with DR.

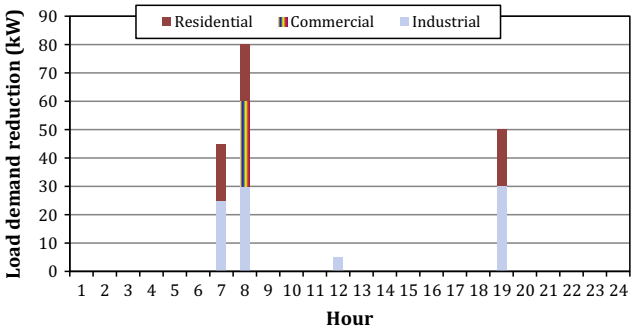

Fig. 11. Scheduled demand curtailment in the case with DR.

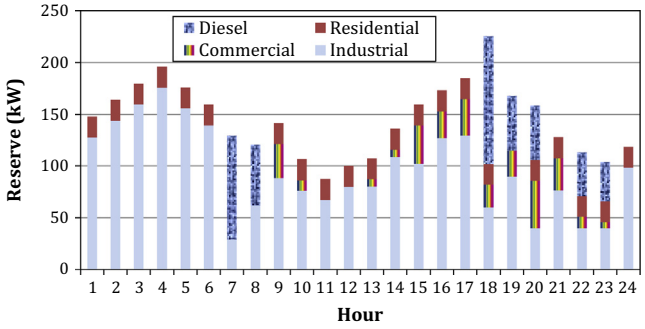

Fig. 12. Scheduled reserve in the case with DR.

Table 6
Computation time vs. accuracy.

Scenario number	Computation time (s)	Discrepancy (%)
4000	23	0
2000	16	0.42
1000	11	0.83
500	5	1.3

reserve. It is worth to mention that in order to provide spinning reserve, a generator should be turned on.

The operational planning is also performed by taken into account DR programs. Figs. 10 and 11 show, respectively, the energy scheduling and load demand reductions. Also, the scheduled reserve is illustrated in Fig. 12.

Fig. 11 evidences that the load demand reductions have been arranged during hours with high electricity prices. This means that the operator purchases load curtailment when the hourly electricity price is high. Moreover, as shown in Fig. 12, the reserve for compensating wind and solar generation variability has been provided by both diesel generators and loads. As a result, the diesel generators are turned off during the hours with low electricity prices.

In order to analyze the effect of the scenario reduction method in the proposed method, the computation time and accuracy of results have been compared in Table 6. In this comparison, it is assumed that the case study with 4000 scenario is the base case and the discrepancy with other cases is compared with the base case. As shown, the operator can select the number of reduced scenario on the basis of a trade-off analysis between the computation time and the accuracy of the results.

6. Conclusions

In this paper, the operational scheduling problem was formulated in accordance with various constraints related to the operation of a MG. The problem formulation includes allocating reserve capacity, optimal battery scheduling, taking into account the uncertainty of the wind and solar power generation. The Latin hypercube sampling method has been used in order to combine and generate different scenarios of wind and solar power generations. The results evidenced that the stochastic method allowed lower reserve requirements if compared with the conventional deterministic method. The inclusion of demand side participation in both energy and reserve scheduling caused a better solution. Moreover, the effect of *K*-means clustering algorithm as a scenario reduction technique has been analyzed and the results evidenced that this method can reduce the computation time of the proposed stochastic method while maintaining acceptable accuracy in result.

References

[1] Eftekharnejad S, Vittal V, Heydt GT, Keel B, Loehr J. Impact of increased penetration of photovoltaic generation on power systems. IEEE Trans Power Syst 2013;28:893–901.
[2] Ortega-Vazquez M, Kirschen D. Estimating the spinning reserve requirements in systems with significant wind power generation penetration. IEEE Trans Power Syst 2009;24:114–23.
[3] Siano P. Demand response and smart grids—a survey. Renew Sustain Energy Rev 2014;30:461–78.
[4] US Department of Energy. Benefits of demand response in electricity markets and recommendations for achieving them. Report to the United States Congress, February; 2006..
[5] Jiayi H, Chuanwen J, Rong X. A review on distributed energy resources and microgrid. Renew Sustain Energy Rev 2008;12:2472–83.
[6] Paolo P, Lasseter RH. Microgrid: A conceptual solution. In: Proc. power electron. specialists conf., June. vol. 6; 2004. p. 4285–90..
[7] Lasseter RH. Control and design of microgrid components. PSERC Final Project Reports..
[8] Bracco S, Delfino F, Pampararo F, Robba M, Rossi M. The university of Genoa smart polygeneration microgrid test-bed facility: the overall system, the technologies and the research challenges. Renew Sustain Energy Rev 2013;18:442–59.
[9] Toshihisa F, Ryuichi Y. Microgrid field test experiences in Japan. In: Proc. Power Eng. Soc. Gen. Meet., Montreal, QC, Canada, June; 2006..
[10] Using Smart Grids to Enhance Use of Energy-Efficiency and Renewable-Energy Technologies – APEC Energy Working Group; 2011..
[11] Energy and Environmental Economic Inc., Value of Distribution Automation applications prepared, PIER Final Project. Report, CEC 500-2007-028; April 2007..
[12] Hernandez-Aramburo CA, Green TC, Mugniot N. Fuel consumption minimization of a microgrid. IEEE Trans Ind Appl 2005;41:673–81.
[13] Koohi-Kamali S, Rahim NA, Mokhlis H. Smart power management algorithm in microgrid consisting of photovoltaic, diesel, and battery storage plants considering variations in sunlight, temperature, and load. Energy Convers Manage 2014;84:562–82.
[14] Marzband M, Sumper A, Domínguez-García J, Gumara-Ferret R. Experimental validation of a real time energy management system for microgrids in islanded mode using a local day-ahead electricity market and MINLP. Energy Convers Manage 2013;76:314–22.
[15] Zhang D, Shah N, Papageorgiou LG. Efficient energy consumption and operation management in a smart building with microgrid. Energy Convers Manage 2013;74:209–22.
[16] Bae S, Kwasinski A. Dynamic modeling and operation strategy for a microgrid with wind and photovoltaic resources. IEEE Trans Smart Grid 2012;3:1867–76.
[17] Motevasel M, Seifi A. Expert energy management of a micro-grid considering wind energy uncertainty. Energy Convers Manage 2013;83:58–72.
[18] Chen C, Duan S, Cai T. Smart energy management system for optimal microgrid economic operation. IET Renew Power Gen 2011;63:258–67.
[19] Khorramdel B, Raoofat M. Optimal stochastic reactive power scheduling in a microgrid considering voltage droop scheme of DGs and uncertainty of wind farms. Energy 2012;45:994–1006.
[20] Chaouachi A, Kamel RM, Andoulsi R, Nagasaka K. Multiobjective intelligent energy management for A microgrid. IEEE Trans Ind Electron 2013;60:1688–99.
[21] Wang M, Gooi HB. Spinning reserve estimation in microgrids. IEEE Trans Power Syst 2011;26:1164–74.
[22] Conti S, Rizzo SA. Modelling of microgrid-renewable generators accounting for power-output correlation. IEEE Trans Power Del 2013;28:2124–33.
[23] Ahn S, Nam S, Choi J, Moon S. Power scheduling of distributed generators for economic and stable operation of a microgrid. IEEE Trans Power Del; in press. doi: http://dx.doi.org/10.1109/TSG.2012.2233773 [2014]..
[24] Zakariazadeh A, Jadid S, Siano P. Economic-environmental energy and reserve scheduling of smart distribution system: a multiobjective mathematical programming approach. Energy Convers Manage 2014;78:151–64.
[25] Zakariazadeh A, Jadid S, Siano P. Stochastic multi-objective operational planning of smart distribution systems considering demand response programs. Electr Power Syst Res 2014;111:156–68.
[26] Al-Mulla A, ElSherbini A. Demand management through centralized control system using power line communication for existing buildings. Energy Convers Manage 2014;79:477–86.
[27] Zehir MA, Bagriyanik M. Demand side management by controlling refrigerators and its effects on consumers. Energy Convers Manage 2012;64:238–44.
[28] Wang D, Ge S, Jia H, Wang C, Zhou Y, Lu N, et al. A demand response and battery storage coordination algorithm for providing microgrid tie-line smoothing services. IEEE Trans Sustain Energy 2014;5:476–86.
[29] Mohsenianrad AH, Leongarcian A. Optimal residential load control with price prediction in real-time electricity pricing environments. IEEE Trans Smart Grid 2010;1:120–33.
[30] Mohsenianrad AH, Wong V, Jatskevich J, Schober R, Leongarcia A. Autonomous demand side management based on game-theoretic energy consumption scheduling for the future smart grid. IEEE Trans Smart Grid 2010;1:320–31.
[31] Molina-García A, Bouffard F, Kirschen DS. Decentralized demandside contribution to primary frequency control. IEEE Trans Power Syst 2011;26:411–9.

[32] Lu N. An evaluation of the HVAC load potential for providing load balancing service. IEEE Trans Smart Grid 2012;3:1263–70.
[33] Kirby BJ. Spinning reserve from responsive loads. Oak Ridge National Laboratory, TN, USA, ORNL/TM-2003/19; 2003..
[34] Wang J, Redondo NE, Galiana FD. Demand-side reserve offers in joint energy/reserve electricity markets. IEEE Trans Power Syst 2003;18:1300–6.
[35] Behrangrad M, Sugihara H, Funaki T. Effect of optimal spinning reserve requirement on system pollution emission considering reserve supplying demand response in the electricity market. Appl Energy 2011;88: 2548–58.
[36] Zakariazadeh A, Homaee O, Jadid S, Siano P. A new approach for real time voltage control using demand response in an automated distribution system. Appl Energy 2014;114:157–66.
[37] Callaway D. Tapping the energy storage potential in electric loads to deliver load following and regulation, with application to wind energy. Energy Convers Manage 2009;50:1389–400.
[38] Wang D, Parkinson S, Miao W, Jia H, Crawford C, Djilali N. Online voltage security assessment considering comfort-constrained demand response control of distributed heat pump systems. Appl Energy 2012;96:104–14.
[39] Lu N, Chassin DP. A state queueing model of thermostatically controlled appliances. IEEE Trans Power Syst 2004;19:1666–73.
[40] Karl Critz D, Busche Sarah, Connors Stephen. Power systems balancing with high penetration renewables: the potential of demand response in Hawaii. Energy Convers Manage 2013;76:609–19.
[41] Castillo-Cagigal M, Gutiérrez A, Monasterio-Huelin F, Caamaño-Martín E, Masa D, Jiménez-Leube J. A semi-distributed electric demand-side management system with PV generation for self-consumption enhancement. Energy Convers Manage 2011;52:2659–66.
[42] Bertoldi P, Atanasiu B. Electricity consumption and efficiency trends in the enlarged European Union. Tech. Rep. EUR 22753 EN, Institute for Environment and Sustainability; 2007..
[43] Hamidi V, Li F, Robinson F. Demand response in the UK's domestic sector. Electr Power Syst Res 2009;79(12):1722–6.
[44] Boyle G. Renewable energy. Oxford, UK: Oxford Univ. Press; 2004.
[45] Borowy BS, Salameh ZM. Optimum photovoltaic array size for a hybrid wind/PV system. IEEE Trans Energy Convers 1994;9:482–8.
[46] Salameh ZM, Borowy BS, Amin ARA. Photovoltaic module-site matching based on the capacity factors. IEEE Trans Energy Convers 1995;10:326–32.
[47] Youcef F, Mefti A, Adane A, Bouroubi MY. Statistical analysis of solar measurements in Algeria using beta distributions. Renew Energy 2002;26: 47–67.
[48] Chedid R, Akiki H, Rahman S. A decision support technique for the design of hybrid solar-wind power systems. IEEE Trans Energy Convers 1995;13:76–83.
[49] Yu H et al. Probabilistic load flow evaluation with hybrid latin hypercube sampling and cholesky decomposition. IEEE Trans Power Syst 2009;24:661–7.
[50] Shu Z, Jirutitijaroen P. Latin hypercube sampling techniques for power systems reliability analysis with renewable energy sources. IEEE Trans Power Syst 2011;26:2066–73.
[51] Baringo L, Conejo A. Correlated wind-power production and electric load scenarios for investment decisions. Appl Energy 2013;101:475–82.
[52] Birge JR, Louveaux F. Introduction to stochastic programming. New York: Springer-Verlag; 1997.
[53] Bouffard F, Galiana FD. Stochastic security for operations planning with significant wind power generation. IEEE Trans Power Syst 2008;23:306–16.
[54] Bouffard F, Galiana FD, Conejo AJ. Market-clearing with stochastic security Part I: formulation. IEEE Trans Power Syst 2005;20:1818–26.
[55] Wood AJ, Wollenberg FB. Power generation, operation and control, book. New York: John Wiley & Sons, Ltd.; 1996.
[56] Cecati C, Citro C, Siano P. Combined operations of renewable energy systems and responsive demand in a smart grid. IEEE Trans Sustain Energy 2011; 2:468–76.
[57] Zakariazadeh A, Jadid S, Siano P. Multi-objective scheduling of electric vehicles in smart distribution system. Energy Convers Manage 2014;79:43–53.
[58] CAT C9 diesel generator set specification <http://www.miltoncat.com/products/NewGenerators/ProductLine/Pages/C9_250-300ekW.aspx>..
[59] Diesel Generators 500REOZVC specification sheet, KOHLER Co. <http://www.kohlerpower.com/onlinecatalog/pdf/g5394.pdf>..
[60] Faisal M, Heikki K. System modeling and online optimal management of microgrid using mesh adaptive direct search. Int J Electr Power Energy Syst 2010;32:398–407.
[61] Bouffard F, Galiana FD, Conejo AJ. Market-clearing with stochastic security-Part II: Case studies. IEEE Trans Power Syst 2005;20:1827–35.
[62] Owner's Manual of the AIR403 Wind Turbine Made by SOUTHWEST Windpower Inc. <http://wind-energy-resources.com/wer_50kw_wind_turbine.html>..
[63] The Solar Power Group Company.<http://thesolarpowergroup.com.au/>..
[64] Willy Online Pty Ltd. <http://wind.willyweather.com.au/>..
[65] Hung DQ, Mithulananthan N, Lee K. Determining PV penetration for distribution systems with time-varying load models. IEEE Trans Power Syst; in press [2014]..
[66] Hourly Ontario Energy Price. <https://www.ieso.ca/imoweb/marketdata/hoep.asp>..
[67] Office of Energy Efficiency. Natural Resources Canada, Energy consumption of household appliances shipped in Canada; December 2005..
[68] Zakariazadeh A, Jadid S. Smart microgrid operational planning considering multiple demand response programs. J Renew Sustain Energy 2014;6:013134.
[69] Zakariazadeh A, Jadid S, Siano P. Stochastic operational scheduling of smart distribution system considering wind generation and demand response programs. Int J Electr Power Energy Syst 2014;63:218–25.